Institute of Physics Publishing Journal of Physics: Conference Series **43** (2006) 804–808
doi:10.1088/1742-6596/43/1/196 7th European Conference on Applied Superconductivity

Design of a linear synchronous motor with high temperature superconductor materials in the armature and in the field excitation system

J M Pina[1,3], M V Neves[1], M D McCulloch[2] and A L Rodrigues[1]

[1] Faculdade de Ciências e Tecnologia, Monte Caparica, 2829-516 Caparica, Portugal
[2] University of Oxford, Dep. Eng. Sci., Parks Road, Oxford OX1 3PJ, UK

[3] E-mail: jpina@dee.fct.unl.pt

Abstract. The high diamagnetism observed in high temperature superconducting (HTS) materials lead to applications involving levitation such as the linear synchronous motor (LSM). Certain features taken into account in conventional LSM design cannot be applied in the HTS case, due to these materials characteristics, such as BSCCO stiffness, when used as armature windings. Also other design features, e.g. slot skewing, which reduces the space harmonics of the air gap magnetic flux density, thus influencing motor performance, plays an important role in final cost. These and other aspects such as the thrust force or the effect of motor control through an inverter are examined in this paper, where the analytical and numerical methodologies involved in the design optimisation of a LSM demonstrator with pre-magnetised YBCO pellets in the field excitation system and BSCCO armature windings are described. Simulation results are also included.

1. Introduction: motivation and motor layout

This work's general goal is the development of an ironless LSM with HTS both in the armature and in the mover. The main objective is to study the technical hitches that arise when using HTS, rather then a specific application. Thrust ripple in a linear synchronous motor is directly related to the spectrum of the magnetomotive force (MMF) produced by armature windings. Windings made by commercial multi-filamentary silver matrix stacked BSCCO tapes (see table 1) show high stiffness, and twisting as with copper wires is not possible, due to limited bending radius. The armature is 60 mm wide and the mover contains trapped field YBCO pellets (40*40*10 mm^3), acting as high flux generators (figure 1). BSSCO windings are expected to produce high MMF.

2. Armature design

Armature variables (see figure 2) are: windings turns, N_t; current amplitude, I_S; winding MMF amplitude, $F_I = I_S.N_t$; slot length, σ; winding length, l_w; MMF pole pitch, τ; and width of the armature active part, w_s. For $N_t = 20$ comes $\sigma = 6$ mm and $l_w = 92$ mm.

2.1. Armature with pure sinusoidal currents

Phase currents are $i_a = I_S \cos(\omega t)$, $i_b = I_S \cos(\omega t - 2\pi/3)$ and $i_c = I_S \cos(\omega t + 2\pi/3)$, where $\omega = 2\pi f$ (rad.s^{-1}), and f (Hz) is the current frequency. Total MMF is written as a series with terms a_n and b_n

Table 1. Length characteristics of the BSCCO tape.

Tape Characteristic	Value (mm)
Average width (including kapton isolation)	4.85
Average thickness	0.30
Minimum bending radius, r_b	40

$$f_{mm}(x,t)=\sum_{n=1}^{\infty}\left(a_n\cos\left(\omega t+n\frac{\pi}{\tau}x\right)+b_n\cos\left(\omega t-n\frac{\pi}{\tau}x\right)\right) \tag{2.1}$$

The first term of the series corresponds to a travelling wave with negative speed in the x axis, while the second term corresponds to another one moving in the positive direction. Fundamental synchronous speed is $v_s=2\tau f$ while other harmonics speed is $v_n=\pm 2\tau f/n$. Factors $k_n=\sin\left(n\frac{\pi}{\tau}\frac{\sigma}{2}\right)\Big/\left(n\frac{\pi}{\tau}\frac{\sigma}{2}\right)$ and $k_{nl}=\sin\left(n\frac{\pi}{\tau}\frac{l_w-\sigma}{2}\right)$ define a_n and b_n, see table 2.

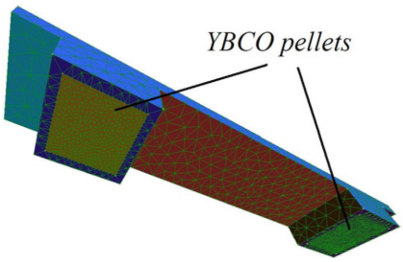

Figure 1. Mover (in 3D Finite Elements).

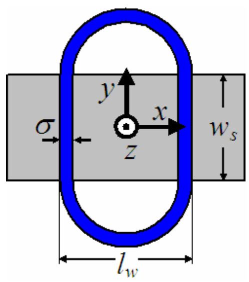

Figure 2. BSCCO winding, with used coordinates.

2.1.1. Topology T_1. It is built by two winding layers and one phase sequence, +A, +C, +B, see figure 3.a). Total MMF, f_{mm}^1, is plotted in figure 4, for $i_a=I_S$. The pole pitch is fixed.

2.1.2. Topology T_2. Phase sequence is +A, −C, +B, −A, +C, −B, see figure 3.b). Total MMF, f_{mm}^2, is plotted in figure 4. Optimum pole pitch is obtained by total harmonic distortion (*THD*) minimization.

2.1.3. Topology T_3. See figure 3.c) for single layer T_3. It must have a double phase sequence, +A, −C, +B, −A, +C, −B. Total MMF, f_{mm}^3, is plotted in figure 4.

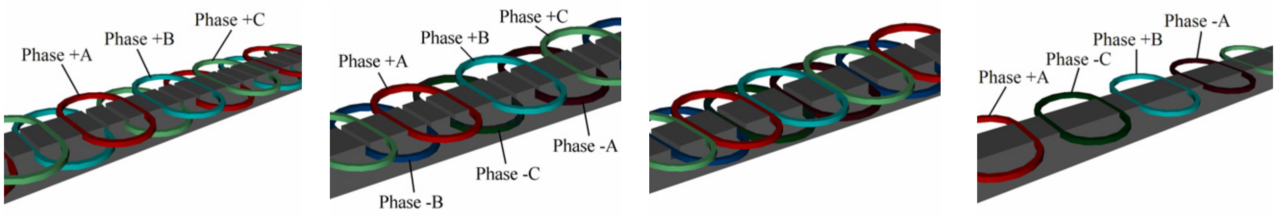

a) Topology T_1. b) Topology T_2 (for different pole pitches). c) Topology T_3.

Figure 3. Different armature topologies.

Table 2. Travelling waves coefficients for different armature topologies.

	Topology T_1	Topologies T_2 and T_3
a_n	$3\frac{F_I}{\pi}\frac{k_n}{n}\sin(n\pi/2), n = 6h-1, h$ natural	$6\frac{F_I}{\pi}\frac{k_n k_{nl}}{n}, n = 6h-1, h$ natural
b_n	$3\frac{F_I}{\pi}\frac{k_n}{n}\sin(n\pi/2), n = 1, n = 6h+1, h$ natural	$6\frac{F_I}{\pi}\frac{k_n k_{nl}}{n}, n = 1, n = 6h+1, h$ natural

2.1.4. Topology selection. The spectra of the different topologies MMFs are compared in figure 5 and main characteristics are pointed out in tables 3 and 4. For the sake of simplicity, T_3 is selected.

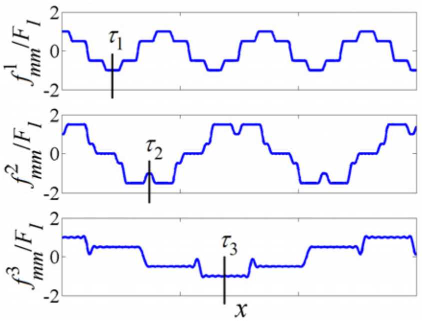

Figure 4. Comparison of MMFs.

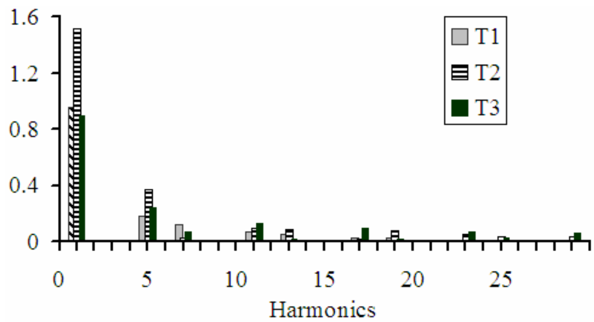

Figure 5. Spectra of the different topologies MMFs (min. THD).

Table 3. Characteristics of the different armature topologies.

	Fundamental's amplitude / F_I	MMF amplitude / F_I	Pole pitch, τ	Minimum *THD* (%)	τ for min *THD* (mm)	Sync. speed v_s, f = 50 Hz (m.s^{-1})
T_1	0.95	1.00	$\tau_1 = l_w - \sigma$	25.0	86	8.6
T_2	1.51	1.74	$1.5l_w \le \tau_2 \le 2l_w + 2\sigma$	26.9	148	14.8
T_3	0.90	1.06	$\tau_3 \ge 3l_w$	35.8	276	27.6

Table 4. Comparison of the different armature topologies.

	Main advantage	Main disadvantage
T_1	Lower harmonic distortion	Fixed pole pitch
T_2	Larger MMF amplitude	High harmonic distortion
T_3	Simplicity of construction	Higher harmonic distortion

2.2. Armature T_3 with rectangular currents

If a current inverter supplies the windings (see figure 6) time harmonics are introduced in MMF

$$f_{mm}(x,t)=\sum_{m=1}^{\infty}\sum_{n=1}^{\infty}\left(a_{m,n}\cos\left(m\omega t+n\frac{\pi}{\tau}x\right)+b_{m,n}\cos\left(m\omega t-n\frac{\pi}{\tau}x\right)\right) \quad (2.2)$$

Harmonic speeds are given by $v_{m,n}=\pm 2\tau f\,\dfrac{m}{n}$. Coefficients $a_{m,n}$ and $b_{m,n}$ are

$$a_{m,n}=(3/2)\cdot F_I a_m^t a_m^x,\ (m=3h \wedge n=3l)\vee(m+n=3h),\ h,l \text{ naturals} \quad (2.3)$$

$$b_{m,n}=(3/2)\cdot F_I a_m^t a_m^x,\ (m=3h \wedge n=3l)\vee(m+n=3h\pm 1 \wedge m\neq 3h \wedge n\neq 3l),\ h,l \text{ naturals} \quad (2.4)$$

where $a_1^t=2\sqrt{3}/\pi$; $a_m^t=\pm\left(2\sqrt{3}/m\pi\right)$, $m=6h\pm 1$, h natural; $a_n^x=(4/n\pi)k_n k_{nl}$, n odd. See figure 7 for MMF spectrum. The MMF and its fundamental are plotted in figure 8. *THD* increased to 48.1%.

3. Trapped-field mover magnets

Trapped-field is calculated by sand-pile model [1]. Discrete current loops carrying constant critical current density J_c are assumed [2]. Using Biot-Savart law flux density is calculated adding all loops contributions, see figure 9 for a single pellet, plane z = 3 mm. J_c = 4000 A.cm^{-1} is used [3].

4. Thrust and lift forces on the mover

Force $\vec{F}$ is calculated by Laplace's law, $d\vec{F}=-I_S d\vec{\ell}\times\vec{B}$, i. e., $dF_x = I_s(B_z)_{av}dy$, for thrust; $dF_z = I_s(B_x)_{av}dy$, for lift. $(B_z)_{av}$ and $(B_x)_{av}$ are the flux density components average over slots height [4]. Contributions of all relevant slots should be considered. I_s = 100 A is used, see figure 10. Unexpected thrust equilibrium angles are found, e. g., $\theta = \pi x/\tau_3$ = 10°, due to reverse magnetic poles around YBCO that align with MMF ones. Commutation angle of 44° maximizes thrust. Thrust oscillations cause speed ripple. Airgap variations, due to lift oscillations, should be minimized by pinning forces.

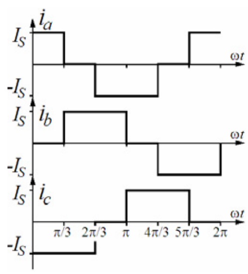

Figure 6. Ideal phase currents.

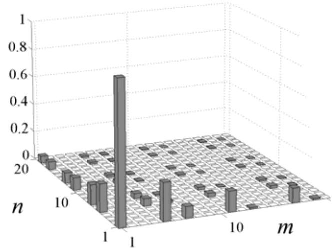

Figure 7. f_{mm} spectrum.

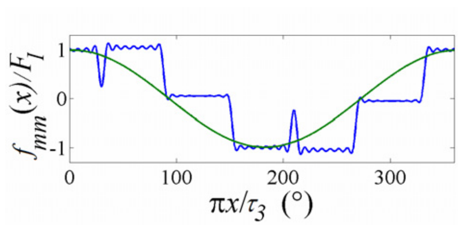

Figure 8. $f_{mm}(x)$ and its fundamental.

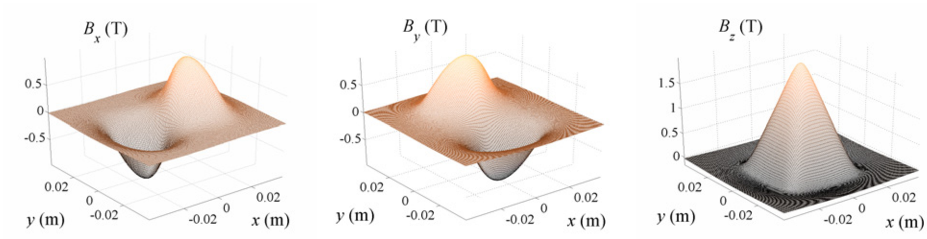

Figure 9. Trapped field components in a YBCO bulk.

5. Slot skewing effect

In conventional motors slot skewing by one slot pitch minimizes induced electromotive force (emf) harmonics. This is not possible with BSCCO tapes. Pole pitch for a skewing angle γ is $\tau_3/\cos(\gamma)$. The electric field generated by the moving magnets with speed $\vec{v}$ is $\vec{E}=\vec{v}\times\vec{B}$. The emf, e, is the integral of this field along the tape, see figure 11 for two angles. Emf minimization is obtained by the minimum of $\varsigma(\gamma)=\int e^2(\gamma,t)dt$ (see figure 12), corresponding to $\gamma \approx 2°$.

6. Conclusions, present and future work

BSCCO physical features restrict its use in winding construction. Flux components perpendicular to tape surface, degrades its critical current [5], preventing the use of LN_2 as cooler. An alternative is to use iron as flux guide, increasing weight. Skew seems to degrade performance, due to slot pitch increase. Although skew generally decreases force ripple, further calculations show that it introduces a lateral force term. Windings are presently being built in nylon moulds in order to start measurements.

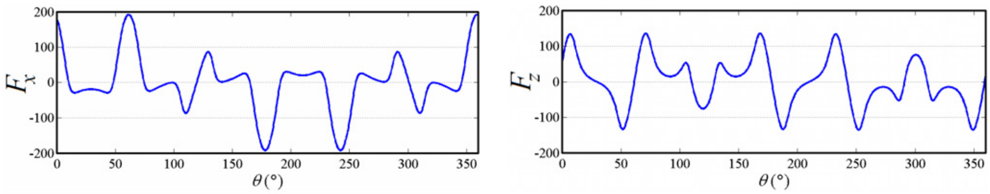

Figure 10. Thrust and lift forces (in N), F_x and F_z, as a function of angle displacement.

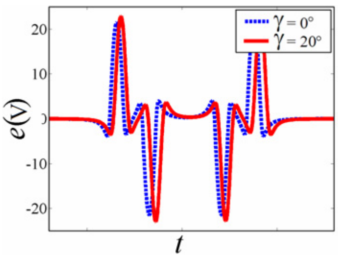

Figure 11. Induced emf in a winding.

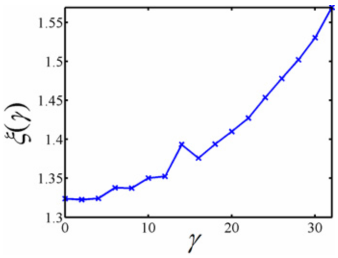

Figure 12. Criterion for emf effect minimization.

References

[1] Aydmer A and Yanmaz E 2005 *Supercond. Sci. Technol.* **18** 1010-15
[2] Bean C 1964 *Rev. Mod. Phys.* **36** 1 31-39
[3] Ren Y, Weinstein R, Liu J, Sawh R and Foster C 1995 *Physica C* **251** 15-26
[4] Boldea I, Nasar S and Fu Z 1988 *IEEE Trans. Mag.* **24** 5 2194-203
[5] Young M, Demko J, Gouge M, Pace M, Lue J and Grabovickic 2003 *IEEE Trans. App. Sup.* **13** 2964-67